Endocytotic potential governs magnetic particle loading in dividing neural cells: Studying modes of particle inheritance

Jacqueline A. Tickle[†], Stuart I. Jenkins[†], Boris Polyak[¥], Mark R. Pickard[†], Divya M. Chari*[†]

[†]Institute for Science and Technology in Medicine, School of Medicine, David Weatherall Building, Keele University, Staffordshire, ST5 5BG, UK

[¥]Department of Surgery and Department of Pharmacology and Physiology, Drexel University College of Medicine, Philadelphia, PA 19102, USA

email: j.a.tickle@keele.ac.uk

s.i.jenkins@keele.ac.uk

Boris.Polyak@drexelmed.edu

m.r.pickard@keele.ac.uk

d.chari@keele.ac.uk *(corresponding author)

Abstract

Aim: To achieve high and sustained magnetic particle (MP)-loading in a proliferative and endocytotically-active neural transplant population (astrocytes) through tailored magnetite content in polymeric iron oxide particles. **Materials & methods:** MPs of varying magnetite content were applied to primary-derived rat cortical astrocytes ± static/oscillating magnetic fields to assess labeling efficiency and safety. **Results:** Higher magnetite content particles display high but safe accumulation in astrocytes, with longer-term label retention versus lower/no magnetite content particles. Magnetic fields enhanced loading extent. Dynamic live cell imaging of dividing labeled astrocytes demonstrated that particle distribution into daughter cells is predominantly 'asymmetric'. **Conclusion:** These findings could inform protocols to achieve efficient MP loading into neural transplant cells, with significant implications for post-transplantation tracking/localization.

Key words: Astrocytes, magnetite, magnetolabeling, cell transplantation, polymeric particles, label dilution

Introduction

Deploying magnetic particles (MPs) with cell therapies for magnetic cell localization and imaging applications is paving the way for safe and efficient delivery of cell transplant populations to sites of pathology, and allowing for non-invasive monitoring of grafts [1–4]. A major emergent area for such applications, given the limited regenerative capacity of the central nervous system, is in neural cell transplantation for the repair of neurological injury and disease. Labeling cells prior to transplantation requires a cell-particle combination that results in rapid and safe particle uptake by the majority of (ideally all) cells. However, the regenerative capacity of most transplant populations relies partially on their proliferative capacity which results in rapid dilution of intracellular particle accumulations in labeled cells [5]. Particle loss can also occur via exocytosis, potentially compromising magnetic cell localization and imaging success [6]. Therefore, a further requirement for transplant cell labeling is long term retention of sufficient particles per cell to confer utility, despite the proliferative nature of the cell, which could be achieved by high initial loading of label into graft cells.

In order to achieve this goal, we require a clear understanding of both the physicochemical and biological parameters that govern particle loading in transplant populations. However, there is a major knowledge gap regarding the factors that contribute to successful ‘magnetolabeling’ and label retention in neural cells. These issues are complicated by the complexity of the architecture of the nervous system wherein multiple cell types are present possessing distinct biological properties. These cell types vary greatly in terms of proliferative and endocytotic capacity, cell-specific modes of intracellular particle processing and susceptibility to particle induced toxicity, requiring detailed characterizations on a cell-by-cell basis for neurological applications [7].

We recently proved that systematic tailored increases in the magnetite content of polymeric particles could significantly enhance cell labeling (>95% cells labeled) in the typically ‘hard-to-label’ transplant population of neural stem cells (NSCs [8]). However, this study did not evaluate the longer term retention of particles of different magnetite content by the labeled cells, or establish the pattern of ‘inheritance’ of particles by daughter NSCs post-proliferation. Furthermore, it is well established that uptake of nanoparticles is mediated via a range of endocytotic mechanisms [9–12]. In this context, it should be noted that NSCs have relatively small cell bodies, elaborate limited amounts of cell membrane and appear in ultrastructural observations to possess comparatively quiescent membranes [13]. How neural transplant cell populations with greater levels of endocytotic activity handle such high magnetite content MPs is unclear, but it can be postulated that such cell/MP combinations can result in greater enhancement of cell labeling for neural transplant applications.

In order to address these issues, we have applied particles with differing magnetite content to cortical astrocytes of primary origin. The astrocytes offer major promise as a transplant population [14–16] and also play key roles in lesion sites post-injury [17]; as such these are of great interest as a target cell population for nanotechnology studies. Astrocytes have major homeostatic functions in the CNS, for example in the maintenance of normal ionic concentrations and neurotransmitter levels in the extracellular space [18,19]. Consistent with these roles, astrocytes display high levels of membrane activity and can mediate nanoparticle uptake via a broad range of endocytotic

mechanisms [19,20]. Indeed, in a recent ultrastructural study using an advanced and high resolution scanning electron microscopy technique, we showed that astrocytes are the dominant neuroepithelial population in terms of particle uptake, displaying extensive membrane ruffling with numerous filopodia/membrane pits in line with greater particle uptake/transfection, relative to other major neural cell types such as neurons and oligodendrocytes [21]; MPs appear to be relatively stable (not degraded) within these cells [7]. Of relevance to the current study, these cells also have a relatively short cell cycle time (ca. 20 h) making these ideal for capture of cell division events and dynamic imaging studies of particle inheritance [22,23]. Polymeric particles with different levels of magnetite content deployed in this study were formulated using biocompatible and biodegradable components highlighting their translational potential and justifying their use in this study [8]. The main study goals were to investigate the influence of tailored particle magnetite content on (i) astrocyte loading and (ii) particle retention, whilst evaluating the safety of the methods, and (iii) to investigate the profiles of particle inheritance in the daughter cells of labeled astrocytes using dynamic time lapse imaging.

Materials & Methods

The care and use of animals was in accordance with the Animals (Scientific Procedures) Act of 1986 (UK), and approved by the local ethics committee.

Astrocyte cell culture

Disaggregated cerebral cortices from Sprague-Dawley rats (postnatal day 1-3) were used to establish mixed glial cultures. Following seven days' culture in D10 medium (Dulbecco's modified Eagle's medium, 2 mM glutaMAX-I, 1 mM sodium pyruvate, 50 U/mL penicillin, 50 µg/mL streptomycin, and 10% fetal bovine serum), sequential overnight shakes facilitated astrocyte purification [24]. Astrocytes were enzymatically-detached (TrypLE synthetic trypsin, Life Technologies), plated on poly-D-lysine (PDL) coated T75 flasks, and maintained in D10 medium, as previously described [25]. Subconfluent cultures were enzymatically-detached by addition of TrypLE

and orbital shaking at 100 rpm, <5 min. Following centrifugation (1000 rpm; 4 min) and phosphate buffered saline (PBS) wash (800 µL), cells were re-suspended in D10 for plating.

Magnetic particle characterization

Superparamagnetic, PLA/PVA coated particles, with a fluorescent BODIPY® 564/570–PLA coating and of differing relative magnetite matrix loading, termed MP-0x (non-magnetite), MP-1x and MP-5x, were prepared by the Boris Polyak Laboratory, Drexel University, Philadelphia, using published procedures [26]. These were formulated using biocompatible and biodegradable components [poly(lactic acid; PLA), poly(vinyl alcohol; PVA), magnetite and oleic acid]. Extensive characterization of these MPs has previously been undertaken [8,27]. In brief, the average sizes are similar for each particle type (hydrodynamic diameter 262-278 nm) with a slightly negative surface charge (-9.5 to -14.4 mV) The differing magnetite content of these particles alters magnetic responsiveness and weight ratio of the MPs, but not particle size or surface charge. FTIR spectroscopy confirmed similar organic composition of each particle type, with no alteration due to increased magnetite loading [8] (Table 1).

Magnetic particle labeling utilizing the magnefect-nano device

The MPs were evaluated for cellular labeling efficiency and extent of cellular accumulation over time. For particle uptake experiments, astrocytes were seeded onto PDL-coated glass coverslips in 24-well plates (0.4×10^5 cells/cm^2), and allowed to adhere for 24 h prior to addition of MPs, followed immediately by exposure to a magnetic field. Lyophilized MPs were re-suspended in sterile water and added to D10 at a concentration of 13 µg (MP-0x), 15 µg (MP-1x) and 26.5 µg (MP-5x) per mL of fresh D10 medium; each corresponding to an identical concentration (particles per mL), as MP density increases with greater magnetite content [8].

Particles were added to cultures (0.3 mL per culture well), with control cultures receiving D10 without MPs. To enhance particle/cell interactions, a magnefect-nano device was used [high gradient neodymium iron boron (NdFeB) magnets with lateral oscillation capability and programmable

frequency/amplitude; field strength at magnet face 421 ± 20 mT (24-magnet array) and 303 ± 5 mT (96-magnet array); nanoTherics Ltd., Stoke-on-Trent, UK]. The superparamagnetic nature of the particles allows for magnetic responsiveness only when particles are exposed to a magnetic field and field gradient. Therefore, deploying a magnetic field and field gradient (permanent NdFeB magnets in this study) beneath the culture plate attracts the particles down to the cell monolayer, while the application of an oscillating field/gradient (termed later as a magnetic field condition for simplicity) theoretically causes particles to move horizontally along the magnet's surface enhancing the likelihood of contact with cells, and/or oscillate *in situ* when attached to cell membrane, thus stimulating endocytotic mechanisms and enhancing cellular MP uptake [20,28–30]. Culture plates were exposed to a static magnetic field (frequency, F = 0 Hz), an oscillating field (F = 1 Hz; 200 μm amplitude) or no magnetic field (NF) for the first 30 minutes of the MP incubation period (either 4 or 24 h; 37°C, 5% CO_2/95% humidified air throughout). Then cells were washed twice with PBS to remove any particles not internalized by cells, and fixed with 4% paraformaldehyde (25 min at room temperature, RT).

Long term particle retention

Particle retention, i.e. percentage of cells labeled and the extent of MP accumulation were monitored over a 21 day period, together with assessment of particle safety. For these experiments, astrocytes were incubated with particles for 24 h, with exposure to magnetic field conditions for the first 30 minutes, as detailed above, followed by PBS washes (x2) to remove non-internalized particles, then fresh D10 medium was added. To facilitate continued proliferation of astrocytes over the long term, coverslips containing MP-loaded cells were transferred to PDL-coated 6-well plates at 96 h, cultured up to day 7 with the coverslip containing cells then transferred to a fresh well at 14 days and cultivated up to 21 days. Cells were maintained in D10 medium with 50% refresh every 2-3 days, with some cultures fixed (PBS wash x2; 4% paraformaldehyde, 25 min, RT) at day 1 and every 4 days thereafter up to day 21 (6 time points in total).

Immunostaining

Cells were immunostained for glial fibrillary acidic protein (GFAP) to enable assessment of culture purity, morphological characteristics and intracellular localization of particles. Cells were incubated in blocker (5% normal donkey serum and 0.3% Triton X-100; 30 min at RT) followed by overnight incubation at 4°C in primary antibody, polyclonal rabbit anti-GFAP (Z0334; DakoCytomation, Ely, UK; 1:500 in blocker). Following two PBS washes (15 min/wash at RT), cells were incubated in blocker (30 min at RT) prior to incubation with secondary antibody (FITC-labeled donkey anti-rabbit, IgG; Jackson Laboratories, USA; 1:200 in blocker; 2-3 h at RT). Coverslips were washed with PBS (3 x 5 min) then mounted with the nuclear stain DAPI (4',6-diamidino-2-phenylindole; Vector Laboratories, Peterborough, UK).

Fluorescence imaging

MP labeling efficiency, extent of particle accumulation and MP intracellular localization, together with culture characteristics and safety assessment, were assessed using fluorescence micrographs. These consisted of four images – fluorescent channels (BODIPY® 564/570-PLA MPs; FITC-GFAP$^+$ astrocytes; DAPI stained nuclei) and phase image (Axio Scope A1 fluorescence microscope, AxioCam ICc1 digital camera and Axiovision software; Carl Zeiss MicroImaging, GmbH, Germany). A standardized exposure time was used for density quantification of BODIPY® 564/570-PLA MPs. For each of the experimental conditions, at least four micrographs, encompassing a minimum of 100 nuclei, were quantified for statistical analyses.

Particle inheritance- dynamic time lapse imaging

Dynamic time-lapse imaging allowed determination of the pattern of particle inheritance in daughter cells of dividing astrocytes [Axio Zoom V16 with AxioCam ICm1 camera and ZEN software (Blue Ed., v.1.1.1.0); Carl Zeiss GmbH, Germany]. Time-lapse images were acquired from transmitted light and BODIPY® 564/570-relevant fluorescence channels for 48 h, post-addition of MPs. Visual observation of time-lapse imaging videos provided counts of symmetrical/non-symmetrical particle inheritance events. A total of 30 mitotic events were recorded (60 daughter cells) and each was

classified as ‘symmetric’ or ‘asymmetric’. The total area occupied by MPs was determined for both daughters, and events were classed as symmetrical inheritance when each daughter cell contained 40-60% of this area, with non-symmetrical defined as >60% in one daughter cell.

Histological analyses of culture properties

Fluorescence micrographs were triple-merged (Photoshop CS5 Extended, Version 12 x32; Adobe, CA, USA) and viewed using ImageJ (NIH USA) to allow quantification of culture and particle uptake characteristics and safety assessments across each experimental condition. Culture purity was determined as the percentage of DAPI-stained nuclei which were $GFAP^+$, with average cell counts determined from the number of nuclei per micrograph. To quantify astrocyte phenotype ratios, each astrocyte was classified based on morphological characteristics [Type 1 (flat, membranous, unbranched) or Type 2 (highly branched, complex cells)]. For each experimental condition, average cell count, distribution of astrocyte phenotype and percentage of pyknotic nuclei (defined as shrunken, fragmenting nuclei) were quantified from fluorescence micrographs.

Integrated density-based technique for unbiased quantification of extent of cellular MP uptake

In terms of quantification of cellular particle uptake, taking average measures of fluorescence (using plate readers) across cultures or assessing iron uptake by quantitative (culture wide) iron assays, assumes an even particle distribution between cells, and whilst arguably appropriate for cell lines (which behave in a relatively homogenous and clonal manner in respect of particle uptake), this approach is *not* suitable for evaluating MP uptake in the astrocyte cultures used in our studies which are derived from primary cortical tissue and show extensive heterogeneity in uptake. Moreover, fluorescence measurements typically include substantial extracellular (membrane-bound) particles (notably, up to 50% of the signal for astrocytes [31]). In this context, a flow cytometry approach was also considered but rejected as particles adherent to the plasma membrane lead to ‘false-positives’. Moreover, enzymatically-detached cells provide few morphological features for analysis, features pertinent to the assessment of uptake and toxicity in specific astrocyte classes. MP labeling

efficiency (% labeled cells) and the extent of particle accumulation within cells, were quantified using triple-merges of DAPI, GFAP and particle images/channels. The dense accumulation of internalized particles prevented exact particle counts per cell, therefore particle accumulation per cell was quantified using integrated density (ID - a measure of pixel intensity) values (ImageJ software, NIH USA). Merged fluorescence micrographs were scaled and, for each MP-labeled astrocyte, the total area per cell occupied by intracellular MPs was outlined, with this outline then being transferred to the un-merged particle channel from which a raw cellular ID measure was obtained. Five background measures were taken from the same un-merged particle channel. The cellular ID values are presented as a corrected total cell fluorescence (CTCF) measure, where:

CTCF = ID – (area of selected cell X mean fluorescence of background readings)

Therefore the resulting CTCF value represents the fluorescence intensity of the internalised particles (having corrected for any background fluorescence) and as such provides a quantifiable and unbiased measure of particle accumulation within the cell.

Statistical analyses

Data were analyzed by one-way ANOVA, with Bonferroni's post-hoc multiple comparison test (Prism software, version 6.03; GraphPad, CA, USA). All data are expressed as mean ± standard error of the mean (SEM) with *'n'* referring to the number of different cultures, each derived from a different rat litter.

Results

Astrocyte uptake characteristics for particles with differing proportions of magnetite: Astrocyte cultures used in our study were of high purity as judged by expression of the astrocyte marker GFAP (99.4 ± 0.2% of cells were $GFAP^+$, $n = 6$). Cells displayed healthy morphologies typical of Type 1 and Type 2 astrocytes (Fig. 1, a), with Type 1 cells dominating (92.4 ± 1.0% of $GFAP^+$

cells). Both perinuclear and cytoplasmic distributions of MPs were observed post-labeling (Fig. 1, a-c). Visual analysis showed widespread cellular uptake throughout cultures for all three particle types, and revealed cellular heterogeneity in terms of relative particle accumulation showing low, medium or high uptake (Fig. 1, a-c).

Particle uptake was rapid, and for magnetite-loaded cells a substantial proportion (ca. 50%) of cells were MP-labeled at 4 h post-particle exposure; MP-5x particles showed significantly increased labeling efficiency versus the other particle types, and in turn, MP-1x showed significantly increased MP-labeling versus MP-0x (Fig. 1, d). By contrast, magnetic field application had no effect on labeling efficiency with MP-0x or MP-1x particles at 4 h. Further, magnetic fields had no effect on the proportion of cells labeled with the MP-5x particles, which was very high (>90%) even under the no magnetic field condition. With regard to the extent of particle accumulation at 4 h, cells labeled with MP-5x particles showed significantly higher particle accumulation compared with MP-0x and MP-1x particles for both magnetic field conditions (Fig. 1,e); fields also resulted in significantly greater accumulation of MP-5x particles versus the no field condition (Fig. 1, e).

At 24 h, a greater proportion of cells were MP-labeled versus 4 h for all particle types (compare Fig. 1, d and f). Notably, for MP-1x and MP-5x particles, virtually all (>98%) astrocytes were MP-labeled (Fig. 1, f); magnetic field application at both frequencies was without effect at this time point. The extent of particle accumulation was also much greater at 24 h compared to 4 h for all magnetite containing particles (compare Fig. 1, e and g; **please note scale difference of *y*-axes**), with particle accumulation significantly higher versus MP-0x (Fig. 1, g). Further, for MP-5x particles magnetic field application promoted particle accumulation (Fig. 1, g) but the effect was not observed for MP-1x.

Long term particle retention analysis: Long term particle retention was studied for magnetite containing particles with applied oscillating fields, which yield optimal MP loading using our protocols. For both MP-1x and MP-5x, substantial label retention (>50%) was evident over 21 days. For MP-1x particles, approximately 92% of cells were labeled at day 1 and this value declined

significantly by day 17 to *ca.* 51% of cells (Fig. 2; a). For MP-5x particles, in contrast, a greater labeling efficiency (ca. 99% of cells) was obtained at day 1, which declined significantly by day 21, albeit with >78% of cells remaining labeled at this time point (Fig. 2, b). A steady reduction in particle retention was noted over the 21 day time period, with considerable heterogeneity observed over cells in terms of extent of particle retention. Visual observations over time for MP-1x showed a clear transition from perinuclear clustering of particles (Fig. 2, c, inset) to a more cytoplasmic distribution (Fig. 2, c, main image) suggesting reverse trafficking of particles. Whilst a similar pattern was seen overall with MP-5x (Fig 2, d, inset), it was noticeable that a sub-population of astrocytes retained large particle accumulations clustered around the nucleus even at 21 days (Fig 2, d, main image). Extent of particle retention was lower for MP-1x than MP-5x particles (compare Fig. 2, e and f: **please note scale difference of *y*-axes**).

Safety assessment of long term particle retention: Long term retention of the particles did not impair the proliferative capacity of astrocytes, with average cell numbers showing a significant increase by day 9 for both MP-1x and MP-5x particles and for both magnetic field conditions, with no significant differences compared to untreated controls at 21 days (Fig. 3, a- b). Culture purity remained at >99% over the 21 days (Fig. 3, c-d). There was no effect of either particles or magnetic field condition on astrocyte phenotype distribution (84.6 ± 0.7% Type 1 compared with 15.4 ± 0.7% Type 2, average across all conditions; Fig. 3, e-f). A small proportion (<2%) of nuclei were pyknotic across all time points; pyknosis was associated with aberrant intense GFAP staining indicative of membrane detaching from the substrate (Fig. 4, a-b). By contrast, using histological analyses, the majority of labeled cells showed no obvious aberrations in GFAP staining or in astrocyte morphologies compared with controls.

Live cell imaging of particle inheritance in dividing astrocytes: To gain further insight into the pattern of particle distribution into daughter cells, astrocytes labelled with MP-5x particles were studied using dynamic time-lapse imaging of proliferating cells (Fig. 5; See Supplementary data for associated video file). This revealed that daughter cells exhibited a predominantly asymmetric profile

of particle inheritance (from 30 mitotic events, 21 were asymmetric compared with 9 showing symmetrical inheritance; Fig. 5, a). Distribution of particles within the parent cell prior to division (Fig. 5, b & f) was predictive of the inheritance profile in daughter cells. Parent cells exhibiting a symmetric perinuclear distribution of particles (Fig. 5, b-d) gave rise to daughter cells with symmetric inheritance of particles (Fig. 5, e), and mitosis of parent cells with asymmetrically-distributed particles resulted in asymmetric inheritance (Fig. 5, i).

Discussion

Here, we have investigated the interaction between the physicochemical properties (specifically, magnetite content) of polymeric iron oxide particles and a highly endocytotic neural cell (the astrocyte). When trying to achieve intracellular particle uptake by transplant populations, two delivery routes can be considered. Either intrinsic 'engulfing' behaviours of cells can be exploited, or the membrane can be temporarily disrupted (e.g. by electroporation or ultrasound bubble stimulation [32]). As the former approach relies on natural biological mechanisms, it can be argued that this offers a safer and more attractive labeling approach, particularly when long term safety (for example post-transplantation into host tissue) is a critical consideration [33,34]. Generally speaking however, the relative endocytotic behaviours of major neural transplant populations have been poorly documented. In turn, the combinatorial interactions of such engulfing mechanisms with the physicochemical properties of particles have received little attention, but remain an important issue when developing neural transplant labeling methods. It can be predicted that the effectiveness of different labeling approaches may vary depending on the cell type and particle deployed, and protocols will need to be tailored for individual cell/particle combinations.

As far as we are aware, the integrated density-based approach that we have utilized has never been applied for quantification of nanoparticle uptake in cells, providing an unbiased, objective approach at the single-cell level whilst allowing for simultaneous evaluation of cellular morphological features and subcellular particle localization. We demonstrate that enhanced magnetite concentration in particles leads to greater particle loading in highly endocytotically active cells. This is associated with longer particle retention (≥ 21 days) versus cells loaded with particles of lower/no magnetite content. Greater labeling efficiency with high magnetite particles within a short time frame is likely attributable to accelerated gravitational particle sedimentation onto cells (due to the increased particle density), similar to the mechanism by which applied magnetic fields enhance *transfection*-grade MP-mediated gene transfer to target cells ('magnetofection'). This technique is now an established experimental procedure, used widely in laboratories in genetic modification protocols

[35], but the compatibility of this approach with a wider range of MPs (e.g. clinical contrast agents or polymeric particles for drug delivery/magnetic cell targeting) is still relatively unexplored. With the magnetic particles studied here, application of static or oscillating fields did not influence the proportions of cells labeled, but significantly enhanced the *extent* of intracellular particle accumulation. Together, our data suggest that a tailored combination of magnetic field application, high magnetite content particles, and longer particle exposure times operate synergistically allowing for greater labeling efficiencies to be achieved. The prolonged retention of higher magnetite content particles is of high relevance for translational applications, where proliferative dilution/exocytosis and label loss are known to be major challenges [5,36]. It is possible that the longer retention is simply related to higher initial loading into cells, but we cannot rule out effects such as slower exocytosis of higher magnetite content particles. The combination of high survival of our transplant populations post-labeling in conjunction with such slower excretion, may serve to reduce the instance of 'false positive' signals, due to secondary uptake by cell populations such as the resident astrocytes and microglial cells in host tissue.

The overall trend in labeling was similar to that seen in NSCs, although magnetic field application did significantly enhance labeling efficiency with low magnetite content particles in the latter [8]. We can speculate that the higher levels of endocytotic activity in astrocytes result in rapid particle uptake and outweigh the benefits of field application, particularly for higher magnetite content particles with more rapid sedimentary profiles. Further, microscopic observations reveal that for a given condition, the intracellular label per cell is greater in astrocytes versus NSCs. The reasons for this may be related to the morphological features and relative endocytotic profiles of the cells. For example, scanning electron micrographs show broad, flattened morphologies for astrocytes with elaboration of large amounts of cell membrane, and surface features suggestive of high cellular membrane activity (Fig. 6a). By contrast, NSCs are bipolar cells with smaller cell bodies, relatively quiescent membranes and less surface area available for particle uptake (Fig. 6 b); additionally label loss appeared to occur rapidly from NSCs (within one week, unpublished observations). Taken together,

our findings highlight the importance of studying the interactions of neural cell type and endocytotic behaviours in conjunction with particle tailoring strategies.

They also indicate the potential benefits of '*endocytosis pre-stimulation*' strategies in enhancing particle uptake, although such strategies are not routinely used currently in labeling protocols. These could include serum starvation [37], growth factor stimulation [38] or mechanical stimulation (as deforming or shear forces may stimulate endocytosis [28]). A less obvious point to note here is the importance of controlling cell densities for such work; in some populations containing actively dividing cells, there is a density dependent inhibition of endocytosis which could negatively impact particle uptake processes [39]. The majority of neural transplant populations are highly proliferative and are usually propagated under growth factor drive, so the optimal cell densities for each cell type must be established and cellular confluence carefully monitored prior to particle addition in labeling protocols for biomedical applications.

The safety of the procedures utilized here was of paramount concern, given the combined variation of multiple parameters (particle properties, magnetic field application and duration of particle exposure). The procedures did not result in acute or long term alterations in magnetolabeled cells, as determined by a spectrum of safety assays assessing survival, proliferative capacity, and cell phenotype. This finding parallels our previous observations in NSCs, highlighting the neurocompatibility of the particles used [8]. The safety profile of these MPs could be attributable to the slow degradation profile of the PLA matrix component (limiting the rate at which iron leaches from degrading particles; rapid leaching is a major correlate of MP toxicity [40,41]), and is also consistent with the observed stability of intracellular MPs in astrocytes [7]. We have used histological analyses to evaluate particle safety, however astrocytes participate in complex signalling pathways and secrete several biomolecules needed for homeostatic function [16,18,19]. More detailed readouts of safety will require combined proteomic and bioinformatic pathway analyses of potential dysregulated processes in magnetolabeled astrocytes, to establish if particular secretory

mechanisms or individual proteins involved in regenerative processes or signalling pathways are perturbed by the labeling procedures.

As far as we are aware, our study is the first to use a dynamic, live cell imaging approach to study the distribution (inheritance) of MPs into the progeny of neural cells derived from primary cultures. Our observations that particle inheritance is largely asymmetric (in that particle distributions are uneven between daughter cells, post-proliferation), are consistent with previous observations in cell lines wherein particle uptake and redistribution to daughter cells after mitosis, is a "*random*" and asymmetric process [5,36,42,43]. The reasons for this uneven inheritance are unclear, but may relate to non-uniform distribution of MPs around the nuclear poles, which we consistently observed in the majority (*ca.* 75%) of labeled astrocytes. In turn, the reasons for this polarized initial distribution are unknown. Nonetheless, we consider that our findings do have significant implications for the use of the MP platform for biomedical applications involving astrocytes, and indeed other proliferative neural transplant populations. Label loss with cell division contributes to reduced efficacy of particle labeling for imaging/targeting applications; however our results indicate that not all transplant cells would be affected similarly in this regard. Unequal inheritance would imply that with each division, the utility of the intracellular MP label would exponentially diminish for a subpopulation of daughter cells. On the other hand, useful levels of labeling would persist in a larger subpopulation for a longer period of time (than would be predicted with symmetric inheritance) resulting in the ability to track overall biodistribution of the cellular graft, even if some cells are lost to the imaging process. Consequently, we believe that an understanding/characterization of the specific modes of particle inheritance in the progeny of a given labeled transplant population, is an important parameter contributing to particle detection, and must be taken into consideration in studies aiming to optimize MP labeling for neural cell therapies. In summary, a wide range of biological and chemical parameters exert an influence on the utility of the MP platform for neural transplantation therapies (Fig. 7) but require systematic investigation. A detailed understanding of the relative importance of

each of these parameters will allow for the tailored development of optimal labeling protocols for translational applications.

Conclusion

We show that initial greater MP cell loading achieved using high magnetite content polymeric particles in highly endocytotic neural cells, leads to enhanced cellular particle retention. The inheritance of particles into daughter cells, studied using dynamic live cell imaging, is predominantly asymmetric/unequal which we consider will have significant implications for tracking of labeled cells in imaging applications.

Executive summary

Effective tracking of neural transplant populations using magnetic particles requires efficient cell labeling

- This involves high initial cellular loading and effective particle retention for clinically relevant periods in labeled populations.
- The synergistic interactions of biological properties such as cellular endocytotic capacity and physicochemical properties such as particle magnetite content in neural cells are not known.

Tailored nanoparticle and protocol design can increase the efficacy of transplant cell-labeling

- Rapid and efficient particle uptake is achieved using particles with high magnetite content versus those with low/no magnetite.
- Higher magnetite particles are also associated with longer term particle retention in cells.
- Applied magnetic fields/gradients did not affect cell labeling efficiency, but did increase *extent* of cell loading for higher magnetite particles.

Most neural transplant populations are proliferative, and cell division dilutes particle label limiting tracking capacity

- Few studies have investigated the pattern of particle ‘inheritance’ into daughter cells post-division.
- Mitosis typically results in asymmetric particle distribution: daughter cells do not inherit equal proportions of particles.
- The implications for such unequal particle distribution remain to be established with complementary MRI studies.

Conclusions

- Our data can provide valuable information to transplantation biologists and materials chemists to develop effective protocols for labeling cell transplant populations.

Supporting information available: Video 1. Time lapse micrographs of astrocyte culture 8 h post-addition of MP-5x particles. Arrows indicate two mitotic events, with examples of both asymmetric (red arrow, upper half, occurring at time-point ~01:50; 70:30 inheritance split) and symmetric (white arrow, lower half, occurring at time-point ~01:32; 50:50 inheritance split) MP inheritance.

Abbreviations: CNS – central nervous system; DAPI – 4',6-diamidino-2-phenylindole; GFAP – glial fibrillary acidic protein; MP – magnetic particle; NdFeB – neodymium iron boron; NSC – neural stem cell; PBS – phosphate buffered saline; PDL – poly-D-lysine; PLA – poly(lactic acid); PVA – poly(vinyl alcohol).

Author information: Correspondence should be addressed to Prof. Divya M. Chari, Institute for Science and Technology in Medicine, School of Medicine, David Weatherall Building, Keele University, Staffordshire, ST5 5BG, UK. d.chari@keele.ac.uk. Tel: +44 1782 733314. Fax: +44 1782 734634.

Funding sources: This work was supported by grants from the BBSRC (DMC) and USA Award Number R01HL107771 from the National Heart, Lung and Blood Institute (BP). SJ was supported by an EPSRC E-TERM Landscape Fellowship (EP/I017801/1).

Conflict of interest: The authors declare that they have no conflict of interest.

Acknowledgments: *Electron micrographs used with kind permission of Alinda R. Fernandes (Fig. 3, a), and Chris F. Adams (Fig 3, b; both Keele University).*

References

1. Jenkins SI, Yiu HHP, Rosseinsky MJ, Chari DM. Magnetic nanoparticles for oligodendrocyte precursor cell transplantation therapies: progress and challenges. *Mol. Cell. Ther.* 2(1), 23 (2014).

* Review of magnetic particle use for neural transplantation

2. Yanai A, Häfeli UO, Metcalfe AL, *et al.* Focused magnetic stem cell targeting to the retina superparamagnetic iron oxide nanoparticles. *Cell Transplant.* 21(6), 1137-1148 (2012).

3. Chen J, Huang N, Maitz MF, *et al.* Guidance of stem cells to a target destination in vivo by magnetic nanoparticles in a magnetic field. *ACS Appl. Mater. Interfaces*. 5, 5976–5985 (2013).

4. Riegler J, Wells JA, Kyrtatos PG, Price AN, Pankhurst QA, Lythgoe MF. Targeted magnetic delivery and tracking of cells using a magnetic resonance imaging system. *Biomaterials* 31(20), 5366–5371 (2010).

5. Kim JA, Åberg C, Salvati A, Dawson KA. Role of cell cycle on the cellular uptake and dilution of nanoparticles in a cell population. *Nat. Nanotechnol.* 7(1), 62–8 (2012).

6. Jin H, Heller DA, Sharma R, Strano MS. Size-dependent cellular uptake and expulsion of single-walled carbon nanotubes: single particle tracking and a generic uptake model for nanoparticles. *ACS Nano* 3(1), 149–58 (2009).

7. Jenkins SI, Pickard MR, Furness DN, Yiu HHP, Chari DM. Differences in magnetic particle uptake by CNS neuroglial subclasses: implications for neural tissue engineering. *Nanomedicine (Lond.)* 8(6), 951–68 (2013).

8. Adams CF, Rai A, Sneddon G, Yiu HHP, Polyak B, Chari DM. Increasing magnetite contents of polymeric magnetic particles dramatically improves labeling of neural stem cell transplant populations. *Nanomedicine NBM* 11(1), 19–29 (2015).

* Examines influence of particle magnetite content on neural stem cell labeling

9. Yameen B, Choi W Il, Vilos C, Swami A, Shi J, Farokhzad OC. Insight into nanoparticle cellular uptake and intracellular targeting. *J. Control. Release* 190, 485–99 (2014).

10. Canton I, Battaglia G. Endocytosis at the nanoscale. *Chem. Soc. Rev.* 41, 2718–2739 (2012).

11. Verma A, Stellacci F. Effect of surface properties on nanoparticle-cell interactions. *Small* 6(1), 12–21 (2010).

12. Kou L, Sun J, Zhai Y, He Z. The endocytosis and intracellular fate of nanomedicines: Implication for rational design. *Asian J. Pharm. Sci.* 8(1), 1–8 (2013).

13. Fernandes AR, Adams CF, Furness DN, Chari DM. Early membrane responses to magnetic particles are predictors of particle uptake in neural stem cells. *Part. Part. Syst. Charact.* Epub ahead of print (2015).

14. Davies SJA, Shih C-H, Noble M, Mayer-Proschel M, Davies JE, Proschel C. Transplantation of specific human astrocytes promotes functional recovery after spinal cord injury. *PLoS One* 6(3), e17328 (2011).

** Demonstrates utility of astrocytes as neural transplant population

15. Davies JE, Huang C, Proschel C, Noble M, Mayer-Proschel M, Davies SJA. Astrocytes derived from glial-restricted precursors promote spinal cord repair. *J. Biol.* 5(3), 7 (2006).

16. Chu T, Zhou H, Li F, Wang T, Lu L, Feng S. Astrocyte transplantation for spinal cord injury: Current status and perspective. *Brain Res. Bull.* 107, 18–30 (2014).

** Reviews utility of astrocytes as neural transplant population

17. Barnett SC, Linington C. Myelination: do astrocytes play a role? *Neuroscientist* 19(5), 442–50 (2013).

18. Abbott NJ, Rönnbäck L, Hansson E. Astrocyte-endothelial interactions at the blood-brain barrier. *Nat. Rev. Neurosci.* 7, 41–53 (2006).

19. Walz W. Role of astrocytes in the clearance of excess extracellular potassium. *Neurochem. Int.* 36(4-5), 291–300 (2000).

20. Pickard MR, Jenkins SI, Koller C, Furness DN, Chari DM. Magnetic nanoparticle labelling of astrocytes derived for neural transplantation. *Tissue Eng., Part C*. 17(1), 89–99 (2011).

21. Fernandes AR, Chari DM. A multicellular, neuro-mimetic model to study nanoparticle uptake in cells of the central nervous system. *Integr. Biol.* 6(9), 855–861 (2014).

22. Környei Z, Czirók A, Vicsek T, Madarász E. Proliferative and migratory responses of astrocytes to in vitro injury. *J. Neurosci. Res.* 61(4), 421–429 (2000).

23. Morrison RS, de Vellis J, Magoun HW. Growth of purified astrocytes in a chemically defined medium. *Proc. Natl. Acad. Sci. U. S. A.* 78(11), 7205–9 (1981).

24. McCarthy KD, de Vellis J. Preparation of separate astroglial and oligodendroglial cell cultures from rat cerebral tissue. *J. Cell Biol.* 85(3), 890–902 (1980).

25. Pickard MR, Chari DM. Enhancement of magnetic nanoparticle-mediated gene transfer to astrocytes by “magnetofection”: effects of static and oscillating fields. *Nanomedicine (Lond.)*. 5(2), 217–232 (2010).

26. MacDonald C, Barbee K, Polyak B. Force dependent internalization of magnetic nanoparticles results in highly loaded endothelial cells for use as potential therapy delivery vectors. *Pharm. Res.* 29(5), 1270–81 (2012).

27. Johnson, B., Toland, B., Chokshi, R., Mochalin, V., Koutzaki, S., Polyak B. Magnetically responsive paclitaxel-loaded biodegradable nanoparticles for treatment of vascular disease: preparation, characterization and in-vitro evaluation of anti-proliferative potential. *Curr. Drug Deliv.* 7, 263–273 (2010).

28. McBain SC, Griesenbach U, Xenariou S, *et al.* Magnetic nanoparticles as gene delivery agents: enhanced transfection in the presence of oscillating magnet arrays. *Nanotechnology* 19(40), 405102 (2008).

29. Adams CF, Pickard MR, Chari DM. Magnetic nanoparticle mediated transfection of neural stem cell suspension cultures is enhanced by applied oscillating magnetic fields. *Nanomedicine NBM* 9(6), 737–41 (2013).

30. Fouriki A, Farrow N, Clements MA, Dobson J. Evaluation of the magnetic field requirements for nanomagnetic gene transfection. *Nano Rev.* 1, 1–5 (2010).

31. Geppert M, Hohnholt MC, Thiel K, *et al.* Uptake of dimercaptosuccinate-coated magnetic iron oxide nanoparticles by cultured brain astrocytes. *Nanotechnology* 22(14), 145101 (2011).

32. Chaudhuri A, Battaglia G, Golestanian R. The effect of interactions on the cellular uptake of nanoparticles. *Phys. Biol.* 8(4), 046002 (2011).

33. Krueger WHH, Madison DL, Pfeiffer SE. Transient transfection of oligodendrocyte progenitors by electroporation. *Neurochem. Res.* 23(3), 421–426 (1998).

34. Guo Z, Yang N-S, Jiao S, *et al.* Efficient and sustained transgene expression in mature rat oligodendrocytes in primary culture. *J. Neurosci. Res.* 43, 32–41 (1996).

35. Plank C, Zelphati O, Mykhaylyk O. Magnetically enhanced nucleic acid delivery. Ten years of magnetofection-progress and prospects. *Adv. Drug Deliv. Rev.* 63(14-15), 1300–31 (2011).

** Comprehensive review of magnetically-assisted magnetic particle delivery

36. Errington RJ, Brown MR, Silvestre OF, *et al.* Single cell nanoparticle tracking to model cell cycle dynamics and compartmental inheritance. *Cell Cycle* 9(1), 121–30 (2010).

37. Geppert M, Petters C, Thiel K, Dringen R. The presence of serum alters the properties of iron oxide nanoparticles and lowers their accumulation by cultured brain astrocytes. *J. Nanoparticle Res.* 15(1) (2013).

38. Kerr MC, Teasdale RD. Defining macropinocytosis. *Traffic*. 10, 364–371 (2009).

39. Davies PF, Ross R. Growth-mediated, density-dependent inhibition of endocytosis in cultured arterial smooth muscle cells. *Exp. Cell Res.* 129, 329–336 (1980).

40. Petters C, Thiel K, Dringen R. Lysosomal iron liberation is responsible for the vulnerability of brain microglial cells to iron oxide nanoparticles: comparison with neurons and astrocytes. *Nanotoxicology* Epub ahead of print (2015).

41. Soenen SJH, Himmelreich U, Nuytten N, Pisanic TR 2nd, Ferrari A, De Cuyper M. Intracellular nanoparticle coating stability determines nanoparticle diagnostics efficacy and cell functionality. *Small* 6(19), 2136–2145 (2010).

42. Rees P, Wills JW, Brown MR, *et al.* Nanoparticle vesicle encoding for imaging and tracking cell populations. *Nat. Methods*. 11(11), 1177-1181 (2014).

43. Summers HD, Brown MR, Holton MD, *et al.* Quantification of nanoparticle dose and vesicular inheritance in proliferating cells. *ACS Nano*. 7(7), 6129–6137 (2013).

* Investigates particle distribution into progeny of dividing cells

Table 1. Physical characterization of magnetic particles.

Magnetic particle	Magnetite content (w/w)	Hydrodynamic diameter (nm)	ζ-potential (mV)
MP-0x	Non-magnetite	267 ± 0.65	-8.98 ± 0.16
MP-1x	11.5 ± 0.98	262 ± 9.56	-9.46 ± 0.14
MP-5x	46.0 ± 1.08	278 ± 1.62	-14.4 ± 0.34

Data from [8, 26].

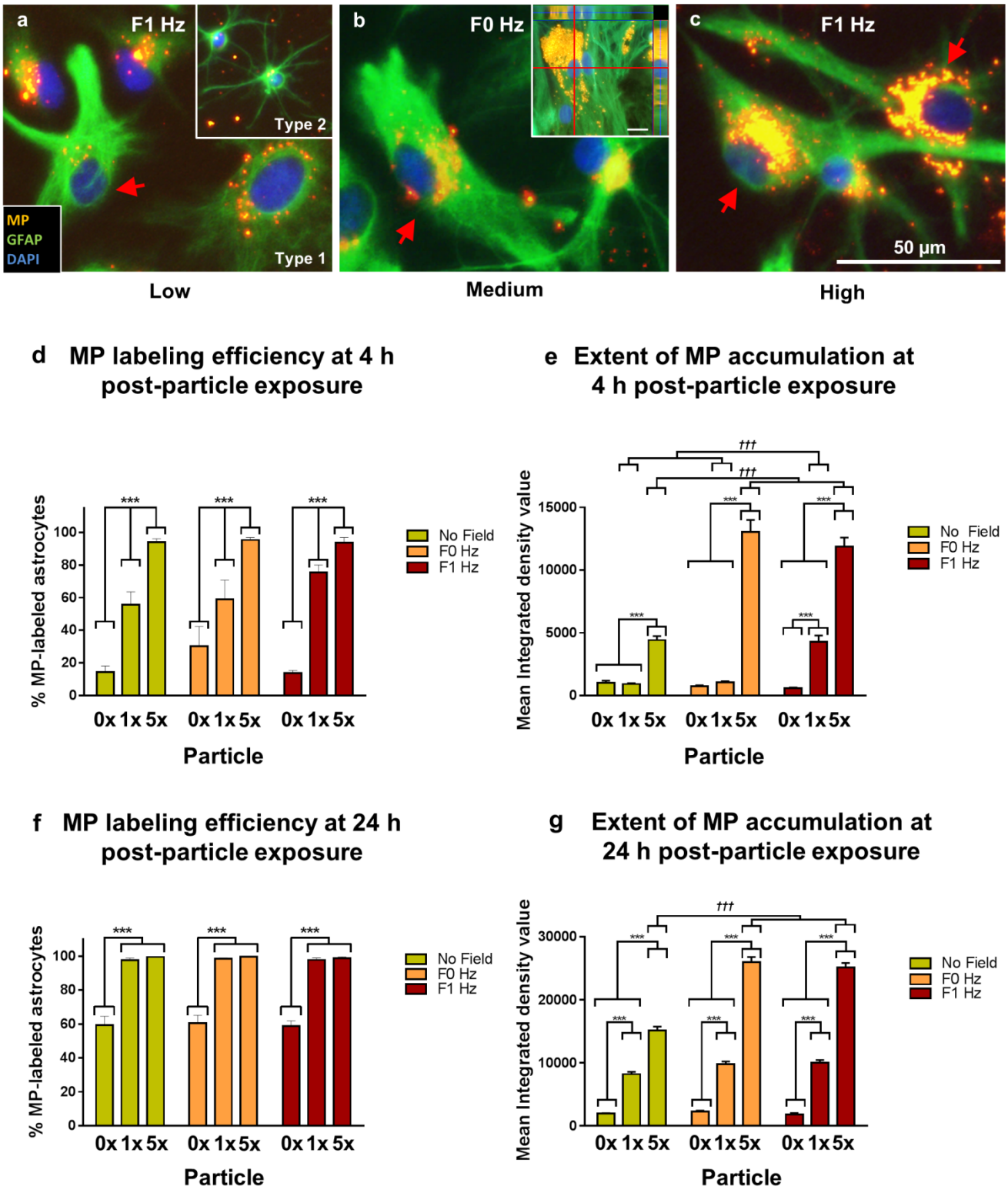

Figure 1. MP-labeling of astrocytes at 4 h and 24 h post-particle exposure, with and without magnetic field application. **(a-c)** Representative triple-merged images of MP-5x particle uptake in Type 1 and Type 2 (a-inset) astrocytes (24 h). Arrows indicate (a) 'low', (b) 'medium' and (c) 'high' levels of intracellular particle accumulation. (b, inset) z-stack micrograph demonstrating intracellular localization of particles. **(d)** Bar chart displaying MP-labeling efficiency in astrocytes at 4 h. **(e)** Bar chart showing extent of particle accumulation across magnetic fields at 4 h. **(f)** Bar chart showing MP-labeling efficiency at 24 h. **(g)** Bar chart showing extent of particle accumulation across magnetic fields at 24 h. Differences are indicated in terms of magnetic field ($^{\dagger\dagger\dagger}P < 0.001$) and particle (*$P < 0.05$, **$P < 0.01$, ***$P < 0.001$). All graphs: $n = 6$.

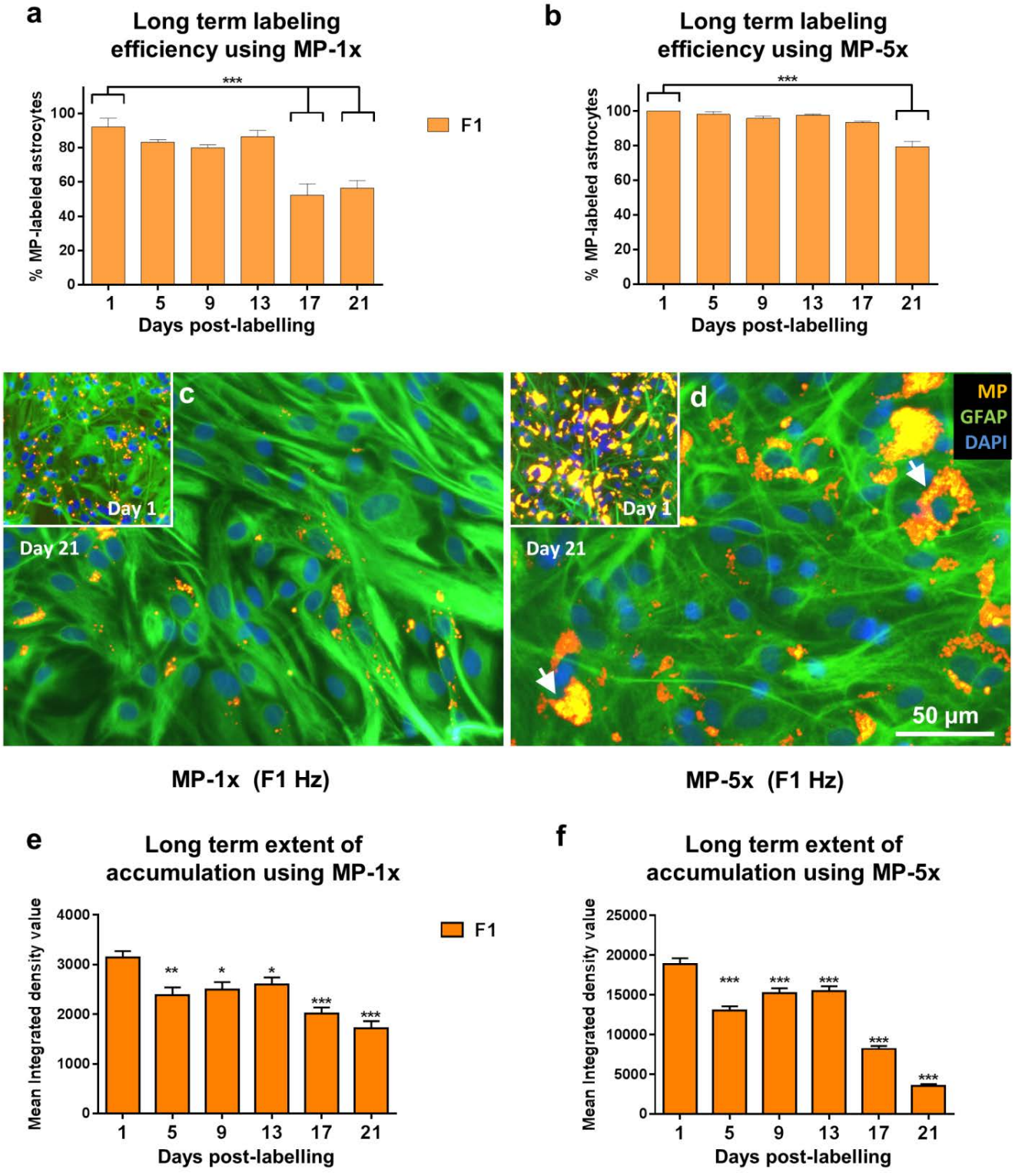

Figure 2. Long term particle retention following 30 min application of an oscillating magnetic field**.** Bar charts showing proportions of labeled cells post-exposure to **(a)** MP-1x and **(b)** MP-5x particles (****P* < 0.001). **(c)** & **(d)** Representative triple-merged images showing differences in levels of particle accumulation seen at day 1 (insets) and day 21 (main images) post-labeling with (c) MP-1x and (d) MP-5x particles. Arrows indicate 'high' levels of perinuclear labeling at day 21 with MP-5x particles. Bar charts displaying levels of **(e)** MP-1x and **(f)** MP-5x particle accumulation over 21 days following exposure to oscillating magnetic field. Within each particle condition, versus day 1:(**P* < 0.05, ***P* < 0.01, ****P* < 0.001). All graphs: *n* = 3.

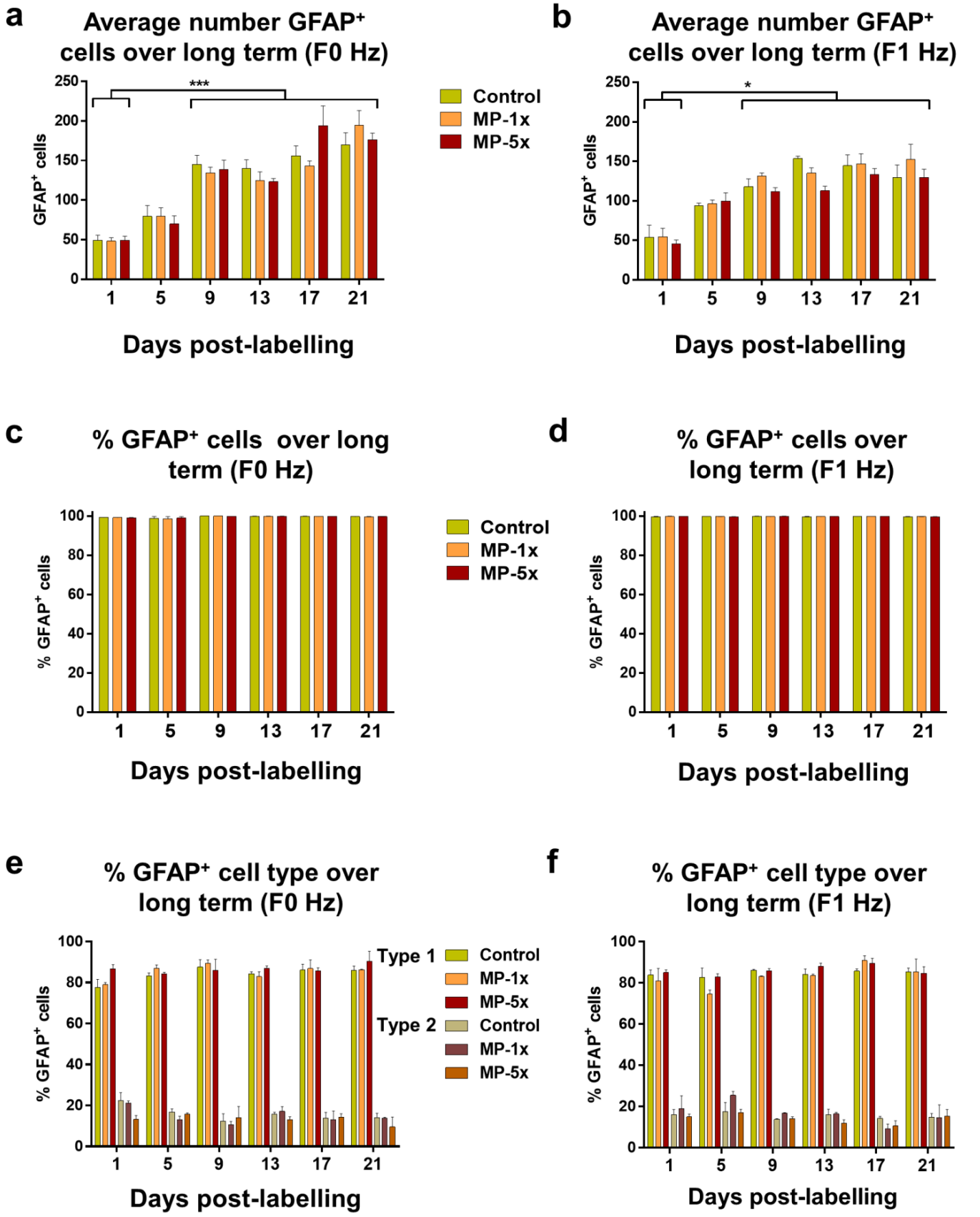

Figure 3. Safety assessment of long term particle retention. Bar charts displaying astrocyte number per microscopic field post-labeling under **(a)** static and **(b)** oscillating magnetic field conditions (*P < 0.05 & ***P < 0.001 versus day 1). Bar charts displaying proportions of GFAP$^+$ cells post-labeling under **(c)** static field and **(d)** oscillating field conditions. Bar charts showing the distribution of astrocyte phenotypes post-labeling under **(e)** static field and **(f)** oscillating field conditions. All graphs: n = 3.

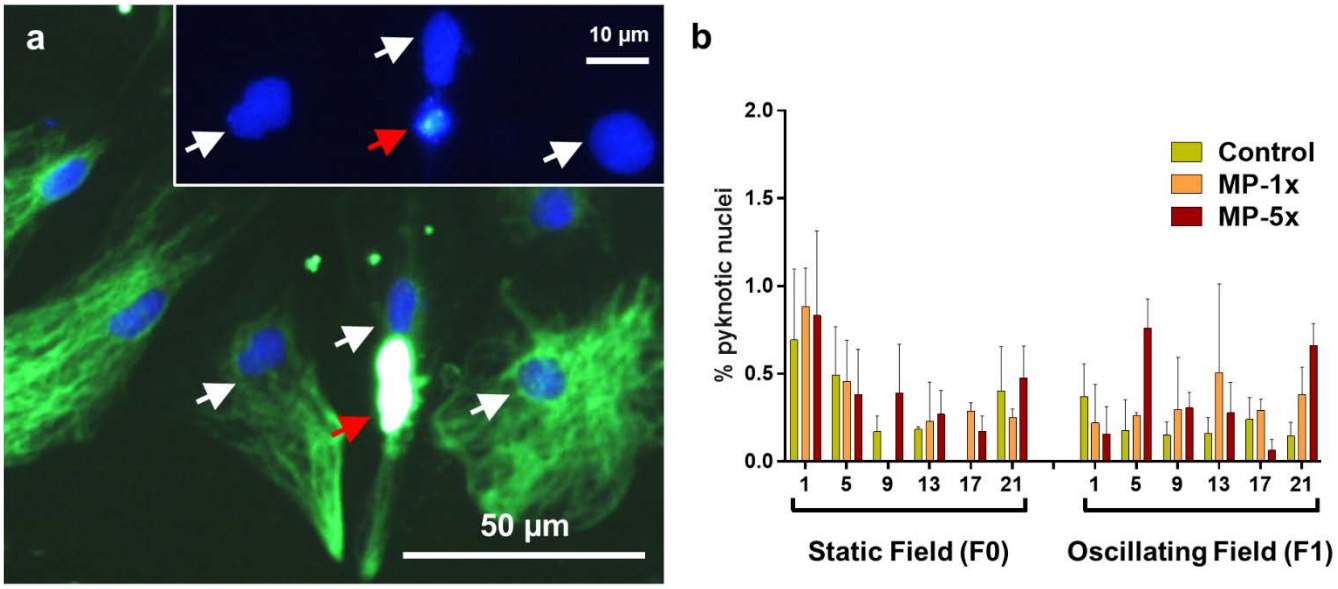

Figure 4. Identification of pyknotic cells in astrocyte cultures. **(a)** The viability of astrocyte cultures was assessed by identifying cells with fragmenting and condensing nuclei, frequently associated with aberrant GFAP staining and evidence of membrane detachment from the substrate, all features indicative of pyknosis (red arrows indicate same pyknotic cell in main image and inset). Healthy nuclei were associated with adherent cells and normal GFAP staining (white arrows indicate same cells in main image and inset). **(b)** The percentage of pyknotic nuclei did not vary across conditions or time-points ($P > 0.05$). All graphs: $n=3$.

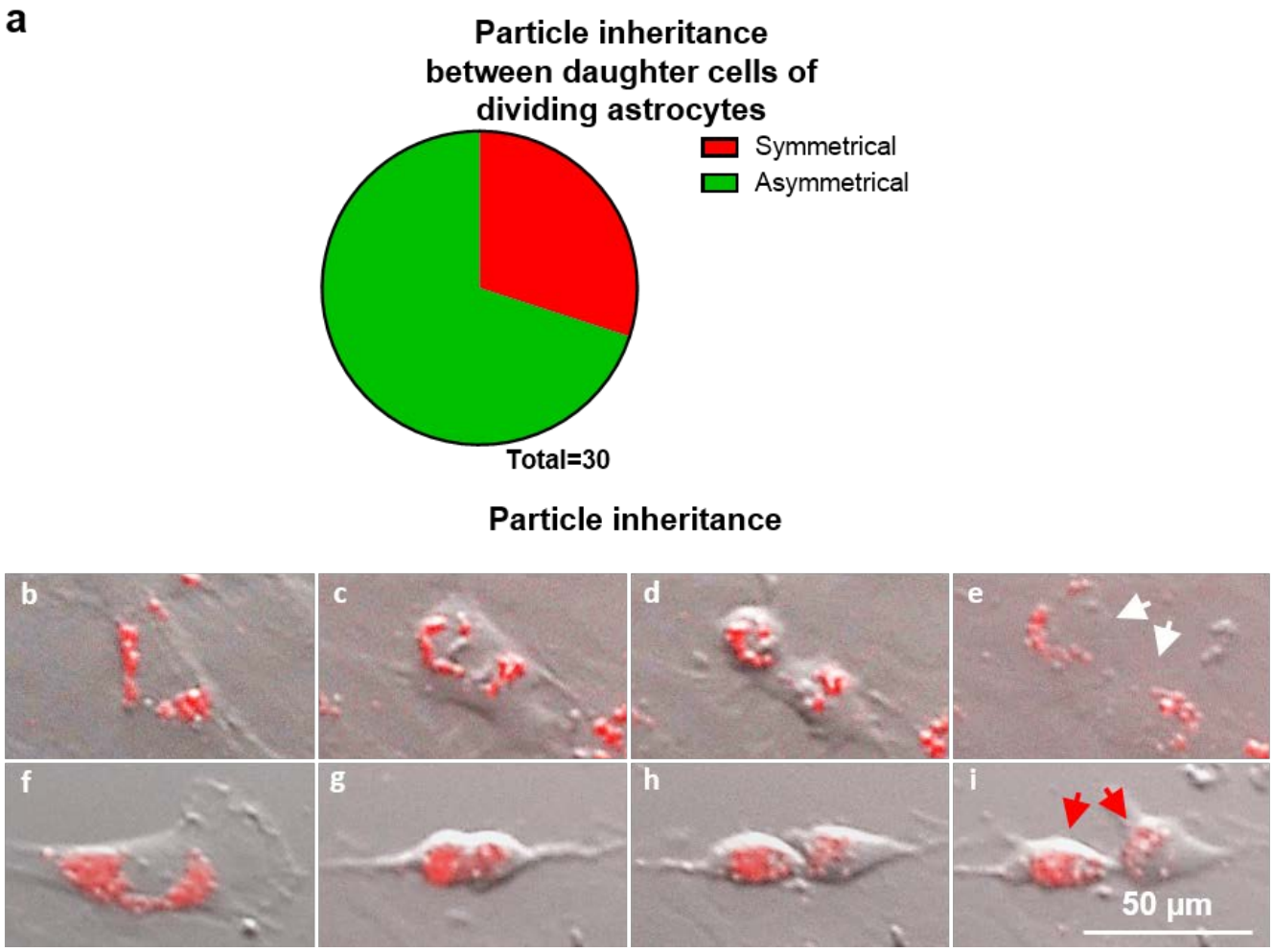

Figure 5. Particle inheritance in labeled astrocytes. **(a)** Pie chart displaying quantification of particle inheritance profiles in MP-labeled astrocytes. **(b) – (i)** Representative sequential still images from dynamic time-lapse imaging (Supplementary data) of dividing astrocytes post- labeling with MP-5x particles without a magnetic field, showing examples of (b-e) symmetric and (f-i) asymmetric particle inheritance between daughter cells (arrows).

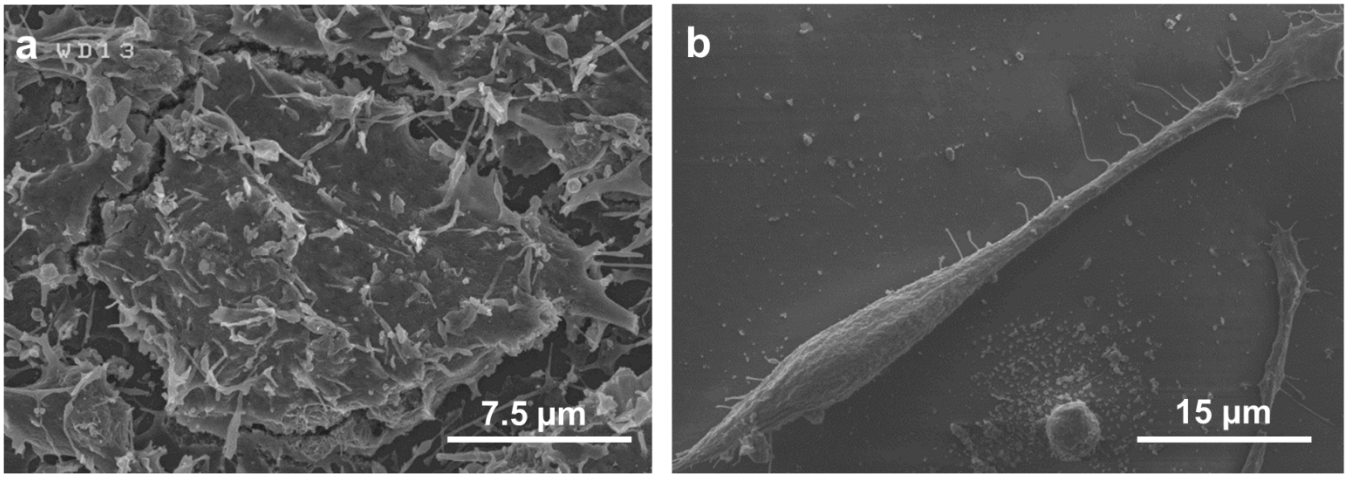

Figure 6. Scanning electron micrographs of **(a)** an astrocyte, and **(b)** a neural stem cell (NSC), for comparison of typical morphological characteristics. Note the differences between the two cell types in terms of both quantity of membrane available for particle interactions, and the quantity of specific membraneous features associated with endocytotic activity, such as processes, filopodia and ruffles. Electron microscopy and NSC culture methods published previously [21].

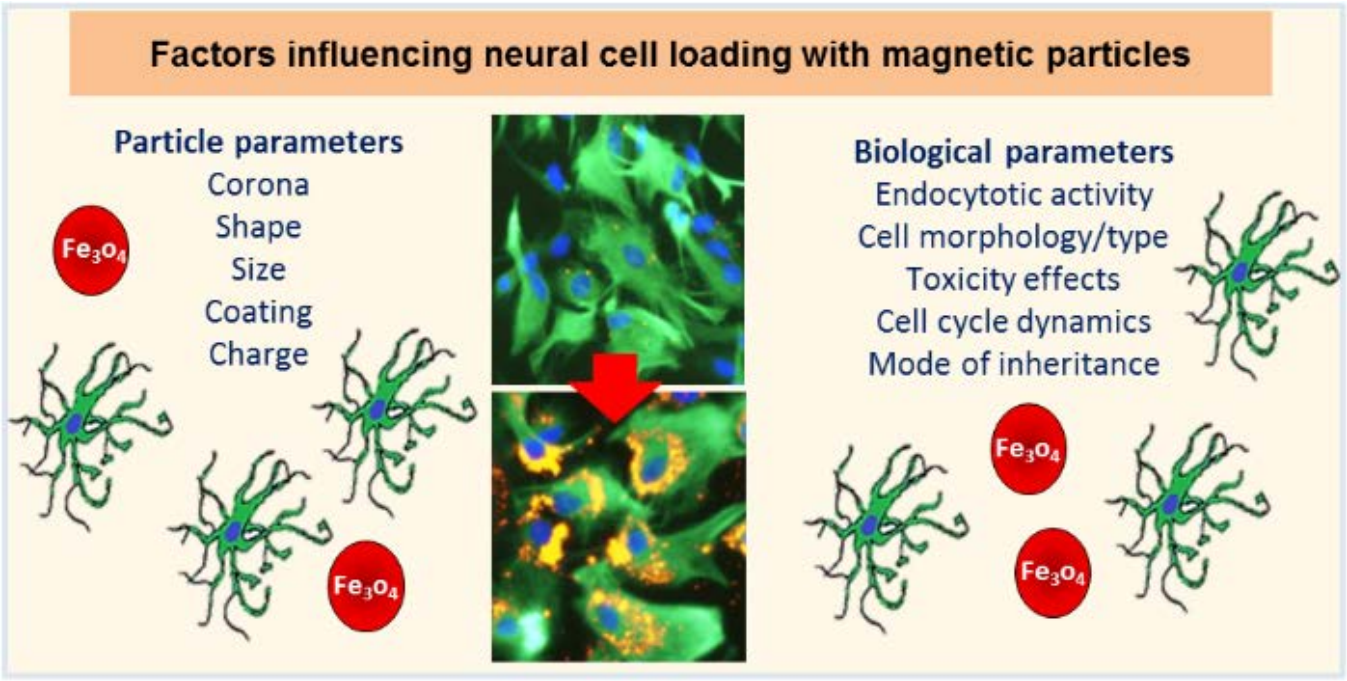

Figure 7. Schematic diagram showing factors that influence cell loading with particles, illustrating the combined dynamics of (i) the physicochemical characteristics of magnetic particles (MPs), and (ii) the biological function of the cell. Micrograph shows MP-5x labeled astrocytes.